Spectral Reflectance Estimation using Wavelet Basis Decomposition

Alamin Mansouri[1], Tadeusz Sliwa[1], Jon Yngve Hardeberg[2], Yvon voisin[1]

[1]Le2i, UMR-CNRS 5158, University of Burgundy, France

[2]Gjøvik University College, Gjøvik, Norway

Abstract

In this paper, we deal with the problem of spectral reflectance functions estimation in the context of multispectral imaging. Because the reconstruction of such functions is an inverse problem, slight variations in input data completely skew the expected results. Therefore, stabilizing the reconstruction process is highly required. To do this, we propose to use wavelets as basis functions and we compare it to Fourier and PCA basis. We present the idea and compare these three methods belonging to the linear model. The PCA method is training-set dependent and confirms its robustness when applied to reflectance estimation of the training sets. Fourier and wavelets basis allow good generalization; an advantage of wavelets being that it avoidsboundary artifacts. The results are evaluated with the commonly used goodness-of-fit coefficient (GFC) and prove the reliability of the use of wavelets.

Introduction

Conventional color imaging defines each pixel with 3 variables such as red, green and blue, which are necessary and sufficient to characterize any color. This principle, the three dimensionality of color, has several limitations. First, in a color image acquisition process, the scene is acquired using a given illuminant. Thus, it is impossible to estimate the scene color accurately under another illuminant. Moreover, two color samples can match under one illuminant and appear completely different under another illuminant. This phenomenon is called metamerism. Multispectral imaging systems remedy these problems by increasing the number of acquisition channels. In doing so, multispectral imaging provides the advantage of high spectral resolution over classical color imaging systems and the advantage of high spatial resolution over spectrophotometers. Furthermore, with such systems, scene surface reflectance recovery from the camera output become easier but not trivial. Thus, finding appropriate mathematical methods to estimate the spectral reflectance from the camera output is a crucial task and of great importance.

Problem formulation

The generally used spectral model of the acquisition chain in a multispectral system is illustrated in Figure 1, where $I(\lambda)$ is the spectral radiance of the illuminant, $r(\lambda)$ is the spectral reflectance of the surface, $o(\lambda)$ is the spectral transmittance of the optical system, $t_k(\lambda)$ is the spectral transmittance related to the k^{th} filter, $c(\lambda)$ is the spectral sensitivity of the camera, and η_k represents the spectral noise for the k^{th} channel, k=1…K.

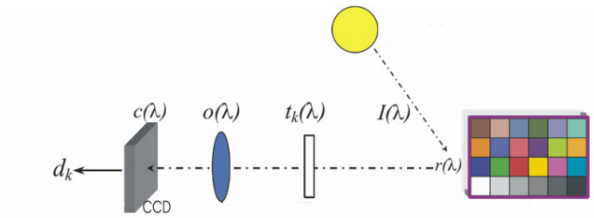

Figure 1. Synopsis of the spectral model of the acquisition process in a multispectral system.

The camera output d_k, related to the channel k for a single pixel of the image, is given by

$$d_k = \int_{\lambda_{min}}^{\lambda_{max}} I(\lambda) r(\lambda) o(\lambda) c(\lambda) t_k(\lambda) d\lambda + \eta_k \qquad (1)$$

If the noise is assumed removed by preprocessing [1], and assuming a linear opto-electronic transfer function, we can replace $I(\lambda)$, $c(\lambda)$, $o(\lambda)$ and $t_k(\lambda)$ by the spectral sensitivity $\mathbf{S}_k(\lambda)$ of the k^{th} channel. Then, the Equation (1) becomes:

$$d_k = \int_{\lambda_{min}}^{\lambda_{max}} S_k(\lambda) r(\lambda) d\lambda \,. \qquad (2)$$

By regularly sampling the spectral range to N wavelengths, Equation 2 can be written in matrix notations as follows:

$$d_k = \mathrm{S}_k^T(\lambda)\mathrm{r}(\lambda)\,, \qquad (3)$$

where $\mathbf{S}_k(\lambda)=[s_k(\lambda_1)\ \ s_k(\lambda_2)\ldots\ s_k(\lambda_N)]^T$ is the vector containing the spectral sensitivity of the acquisition system related to the k^{th} channel, $r(\lambda)=[r(\lambda_1)\ r(\lambda_2)\ldots\ r(\lambda_N)]^T$ is the vector of the sampled spectral reflectances of the scene, and ^{T} is the transpose operator. Considering the system with all channels, Equation 3 can be written as:

$$\mathrm{d} = \mathrm{S}^T\mathrm{r}\,, \qquad (4)$$

where $\mathbf{d}$ is the vector containing all d_k camera outputs and $\mathbf{S}=[\mathbf{s}_1\ \mathbf{s}_2\ldots\ \mathbf{s}_K]^T$ is the matrix containing the channels spectral sensitivities $\mathbf{S}_k$. The final goal is to recover $\mathbf{r}(\lambda)$ from the camera output according to Equation 4. This is obtained by finding an operator $\mathbf{Q}$ that solves for the following equation:

$$\mathrm{r} = \mathrm{Qd}. \quad (5)$$

Depending on how the operator **S** is determined, two paradigms of spectral reflectance estimation exist [2].

- If **S** is obtained by a direct physical system characterization. The operator **Q** is the inverse of **S**. However, **S** is a not usually a square matrix, its inverse does not exist. Only a pseudo-inverse could be calculated. Thus **Q**=pinv(**S**).
- If **S** is obtained indirectly by matching a set of *M* color patches (for which we know the theoretical reflectances) and we capture an image of these patches with the multispectral camera, we have then a set of corresponding pairs ($\mathbf{d}_m$, $\mathbf{r}_m$), for m=1,...,M, where $\mathbf{d}_m$ is a vector of dimension K containing the camera responses and $\mathbf{r}_m$ is a vector of dimension N representing the spectral reflectance of the m^{th} patch. The reflectances $\mathbf{r}_m$ are gathered in the matrix **R** and the camera outputs for the M patches are gathered in the matrix **D**. The operator **Q** is straightforwardly obtained by calculation of this matching. Any optimization method can fulfill this aim (neural networks, Least squares…). Thus, the operator **Q** is obtained like:

$$\mathrm{R} = \mathrm{QD} \quad (6)$$

involving then the inversion

$$\mathrm{Q} = \mathrm{RD}^{-1} \quad (7)$$

A third paradigm for spectral reflectance estimation consists of direct interpolation of the camera outputs d_k. Then, no knowledge about operator **S** is required. Nevertheless, rigorous conditions about filters' shape, as well as well calibrated and normalized data is required for this kind of reconstruction. The reconstruction is performed by any interpolation operator (spline, etc.)

The final goal is to estimate spectral reflectance functions **r** from camera outputs **d**. To do so, several methods belonging to the two first paradigms exist in literature [3-5]. Some classical approaches use the pseudo-inverse calculus and the least squares. The main drawback of these methods is instability of solutions due to the noise amplification. That is why some other methods add some constraints on the reflectance functions to be in the range [0 1] or seek to maximize the smoothness of the estimated result [6, 7]. We can also cite a learning-based method using a non-linear neural network [8].

Reflectance estimation in the linear model

Utilization of a linear model to estimate reflectance from camera response seems to be trivial since we supposed a linear opto-electronic transfer function enabling us the matrix notation in Equations 4, 5. Moreover, the linear model offers an alternative to imposing smoothness on reflectance functions [9]. This is expressed by assuming that $\mathbf{r}(\lambda)$ can be approximated by a linear combination of a small number of basis functions [10]. Thus, a set of basis functions B_j (j=1…n) are defined such that each reflectance $\mathbf{r}_i$ could be written as:

$$\mathrm{r}_i = B_j a_{i,j}, \quad (8)$$

where $a_{i,j}$ is the weight of the j^{th} basis function related to the i^{th} sample. The basis functions are themselves functions of wavelength but free of constraints such as being positive or constrained to be limited to the range [0 1]. Their number n is chosen to conserve maximum of energy. Equation 4 can be written as:

$$\mathrm{d} = \mathrm{S}^T\mathrm{Ba}, \quad (9)$$

where the columns of the NxK matrix **B** contain the M basis functions of a linear model of reflectance spectra and the Kx1 matrix a holds the weights that define the particular spectrum that we are trying to reconstruct. When gathering $\mathbf{S}^T$ and **B** in a unique operator, the latter is a square matrix that could be easily inverted. We can rewrite Equation 9 as:

$$\mathrm{a} = (\mathrm{S}^T\mathrm{B})^{-1}\mathrm{d}, \quad (10)$$

which allows us to compute **a**. Afterwards we can easily estimate **r** by simple multiplication:

$$\mathrm{r} = \mathrm{Ba}. \quad (11)$$

In this context, methods belonging to the second paradigm use techniques of decomposition, although implicitly. We can cite the method proposed [11] which takes advantage of the a priori knowledge about the spectral reflectances that are to be imaged (pigments reflectance for paintings reflectance reconstruction). Methods based on linear neural networks are also methods taking benefits from basis decomposition [12]. In our paper we will achieve the decomposition task by experimenting with three basis functions: PCA, Fourier and Wavelets analysis. In the next sections we present the principle of these methods.

PCA analysis

Principal component analysis (PCA) is a technique extensively used for dimensionality reduction in a data set. It consists of finding an orthogonal basis composed of vectors called principal components. Each component is associated to an energy that indicates the statistical relevance of the vector in the data. Technically speaking, PCA is an orthogonal linear transformation that transforms the data to a new coordinate system such that the greatest variance by any projection of the data lies on the first coordinate (called the first principal component), the second greatest variance on the second coordinate, and so on. In the field of multispectral imaging, PCA has been largely used for data compression [13] but also in spectral reflectance reconstruction [14, 15].

In the discrete domain, PCA corresponds to the Karhunen-Loève transform, and could be calculated using Singular Value Decomposition (SVD) [14, 15]. Thus, the basis functions that describe a particular set of reflectances can be obtained. Given an MxN matrix **R** that contains M spectra each, sampled at N wavelengths, we obtain the following decomposition:

$$\mathbf{P} = \mathbf{UWV}^{\mathrm{T}}, \quad (13)$$

where **U** and **V** are MxM and NxN matrices containing the eigenvectors of the matrices $\mathbf{PP}^{\mathrm{T}}$ and $\mathbf{P}^{\mathrm{T}}\mathbf{P}$, respectively. The matrix **W** is an MxN matrix where diagonal entries represent singular values of **P**. The columns of **U** may be used as the basis functions. If all basis functions are used to reconstruct a particular spectrum from the training set, this will yield a perfect reconstruction. However, the interest of using PCA is that it is possible to keep only the most relevant components since it is well known that typically, about 95% of the energy is contained in the three first components [14].

Fourier analysis

To perform a Fourier analysis, we use the Fourier transform. This is based on the assumption that it is

possible to take any periodic function of time and write it as equivalent to an infinite summation of cosine and sine waves with frequencies as integer multiples of base frequency f, $f = 1/T$, where T is the period of the function). We use Fourier transform implemented by the FFT (Fast Fourier Transform) which decomposes a signal into its phase and frequency components. We consider a given reflectance function, one decomposes this function into a sum of basis function written as:

$$B(\lambda) = b + A\cos(2\pi f\lambda + \varphi), \quad (14)$$

where the function B is entirely determined by the value of its offset b, its amplitude A, its frequency f and its phase φ. In this way, the Fourier transform is a linear operator that maps functions to other functions. In a certain way, the Fourier transform decomposes a function into a continuous spectrum of its frequency components, and the inverse transform synthesizes a function from its spectrum of frequency components.

Wavelets analysis

In order to extract information not readily available from the time (wavelength) domain representation it is useful to project the function onto a set of basis functions. The basis functions are those building blocks and the transform determines how those blocks are combined to build the function. The Fourier transform provides tools for studying global function properties — properties that are constant throughout the function — i.e. properties that are stationary. In order to study local or transient function characteristics, Gabor [16] formulated a windowed Fourier transform which correlates a function with time-frequency atoms (STFT). But wavelets transforms often give a better signal representation using Multiresolution analysis. Wavelet analysis refers to the representation of a function in terms of scaled and translated copies (known as daughter wavelets) of a finite length or fast decaying oscillating waveform (known as the mother wavelet). So, a given reflectance spectra r could be decomposed into a wavelet basis $\Psi(\frac{\lambda - a}{b})$ and $\varphi(\frac{\lambda - a}{b})$, where Ψ is the wavelets function at the scale 0 and φ is the scaled associated function. b and a are respectively scale and translation factors.

Experiments and results

In this section, we describe three experiments to evaluate the spectral reflectance estimation performance for the three methods: PCA, Fourier and wavelets analysis. The data we used are sampled at 10nm intervals in the range [400 700] yielding for each spectrum $\mathbf{r}(\lambda)$ to a vector of 31 values.

The aim of this experiment is to derive a small number of basis functions from a set of spectra using the three methods. Then, we try to reconstruct all the set using only the basis we computed. To do this we used a set of 404 natural spectra [14]. We performed decomposition using the three methods. We found that 95% of energy is hold by the six greatest vectors. Furthermore, for practical reasons that involve the number of Fourier and wavelets basis to be multiple of two, we chose to keep the eight first basis functions. The wavelets we used in this paper is the Haar family which is short support and threrefore adapted to our spectra (only 31 values) followed by a post-regularization. Figure 2 depicts the eight basis functions derived from the 404 sample set for the three methods.

Reconstruction of training set

After deriving the basis functions for the "training" set, we try to reconstruct all the spectra in this set using these basis functions and the coefficients matrix **a** (Equation 10). The Figure 3 shows the results for the three methods in terms of visual comparison of reconstructed curves:

We also evaluate the reflectance estimation in terms of an objective metric. For this purpose, we used the non centered correlation coefficient, largely used and known in the community as Goodness of Fit Coefficient (GFC) expressed by the formula:

$$GFC = \frac{\left|\sum_j R_m(\lambda_j) R_r(\lambda_j)\right|}{\left(\left|\sum_j [R_m(\lambda_j)]^2\right|\right)^{1/2} \left(\sum_j [R_r(\lambda_j)]^2\right)^{1/2}}$$

where $R_m(\lambda_j)$ is the value measured by the spectrophotometer in the wavelength λ_j, and $R_r(\lambda_j)$ represents the reconstructed value related to the same wavelength. Table 1 give the full results for the 404 spectra in terms of mean, median, standard deviation and the minimal value of GFC.

Method	GFC			
	Mean	**median**	**STD**	**Min**
PCA	***0.9997***	***0.9999***	***$5.1903.10^{-4}$***	***0.9953***
Fourier	0.9841	0.9905	0.0170	0.8799
Wavelets	0.9952	0.9978	0.0053	0.9655

Table 1: results, in terms of GFC, of the reconstruction of the training set for the three methods

Generalization performance

From the previous results, we retain PCA and Wavelets to test them in the task of generalization. That means we extract a PCA and wavelets basis functions from a set that we call training set and try to estimate reflectance from another set. In our case, we used Macbeth DC as a training set and Macbeth Color checker as reconstruction target. Figure 4 depicts some samples of the performed reconstruction allowing for visual comparison of the reconstructed curves. We also evaluate the generalization capabilities of these two methods in terms of GFC. Table 2 gives the results.

Method	GFC			
	Mean	**median**	**STD**	**Min**
PCA	0.9971	***0.9990***	0.0048	0.9820
Wavelets	***0.9980***	0.9986	***0.0021***	***0.9922***

Table 2: results, in terms of GFC, of the generalization capabilities for the methods using PCA and wavelets basis functions

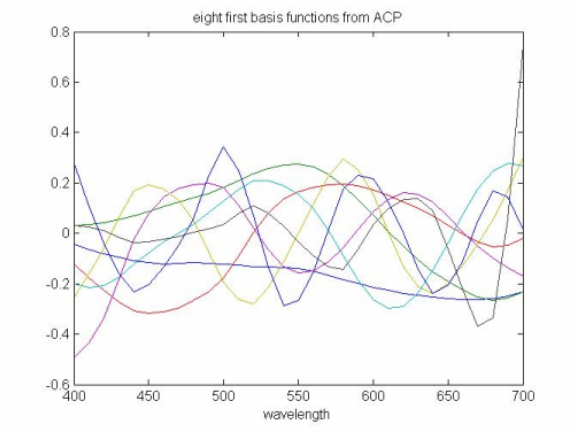

a.

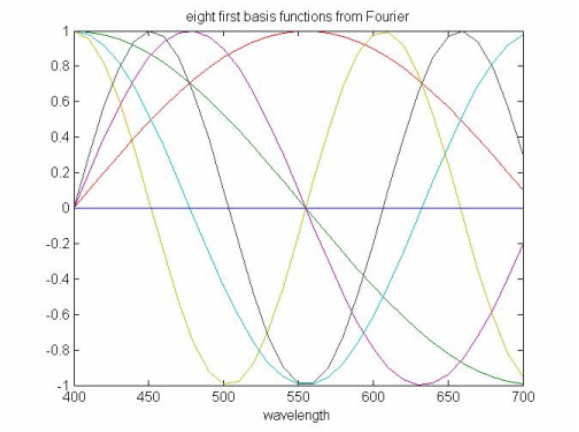

b.

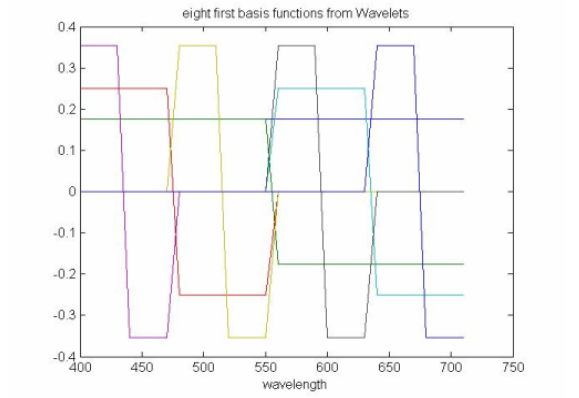

c.

Figure 2: The determined eight basis functions from the set of 404 natural spectra for: a. PCA basis functions where the mean was subtracted, b. Fourier basis functions and c. Wavelets basis functions.

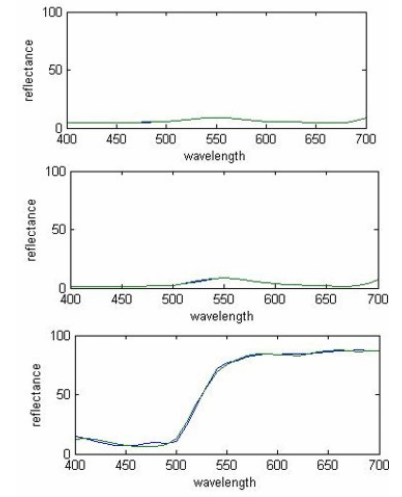

a.

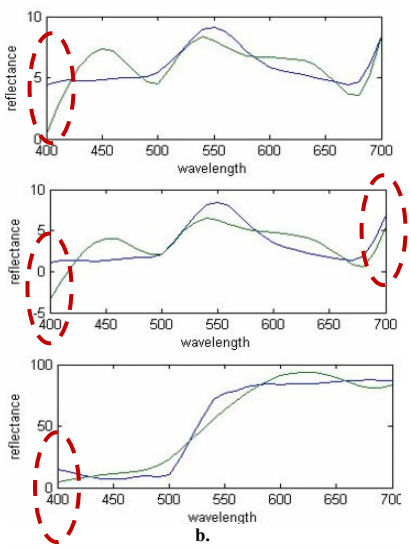

b.

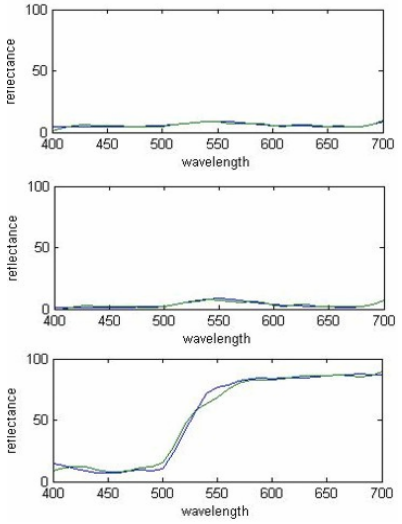

c.

Figure 3: samples of reconstructed spectra from the training set using: **a.** PCA eight basis functions, **b.** Fourier eight basis functions, c. Wavelets eight basis functions.

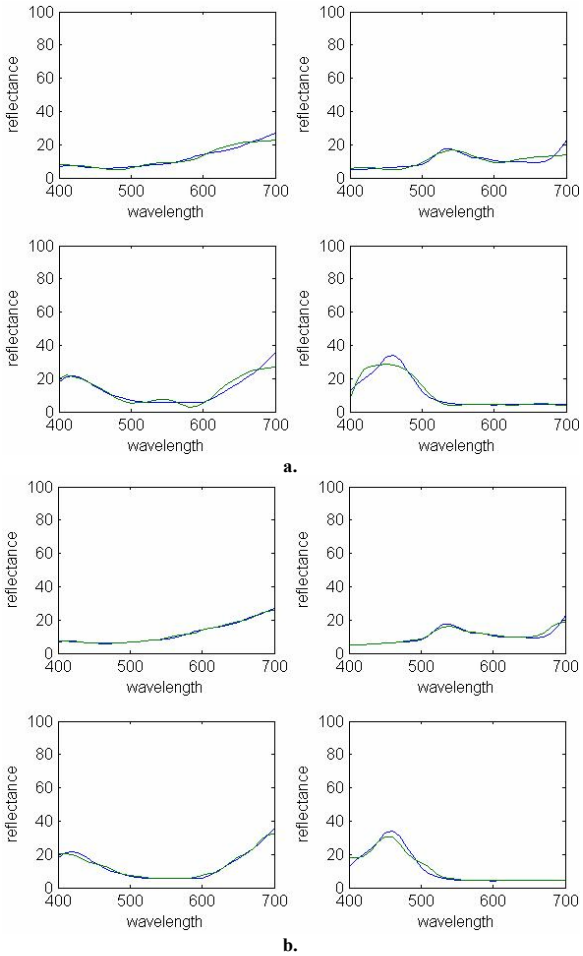

Figure 4: results of generalization test for: a. PCA basis functions and b. Wavelets basis function.

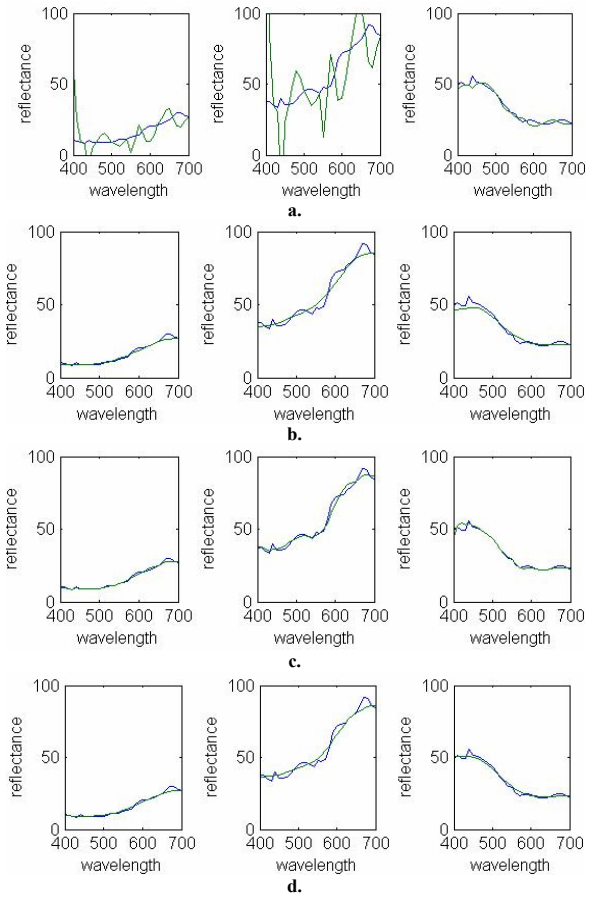

Figure 5: results of reflectance estimation from: a. narrow-band multispectral image using PCA, b. narrow-band multispectral image using wavelets, c. medium-band multispectral image using PCA, and d. medium-band multispectral image using wavelets

Estimation from multispectral image

The main objective in multispectral imaging is to be able to reconstruct full spectral reflectance curves $\mathbf{r}(\lambda)$ from a small number of channels K contained in the vector $\mathbf{d}_k$. That is why we perform this third experiment. We used two multispectral images of the Macbeth DC composed of eight channels representing captured each 40nm in the range [400 700]. The difference between the two images is the shape of the filters. The first image is issued from narrow-band filters, while the second image is issued from medium-band filters (FWHM of 40nm). Then, in order to recover the full spectrum for each patch, we used the previously computed basis in the case of the wavelets but we computed a new basis for the PCA method. Figure 5 shows results for this experiment in terms of visual comparison of curves.

Table 3 gives the results for this experiment in terms of GFC when using a multispectral image issued from narrow band filters.

Method	GFC			
	Mean	**median**	**STD**	**Min**
PCA	0.8841	0.9605	0.1898	0.2847
Wavelets	***0.9948***	***0.9972***	***0.0064***	***0.9710***

Table 3: results, in terms of GFC, for the reflectance estimation from camera outputs in the case of multispectral image from narrow-band filters.

Table 4 gives the results for this experiment in terms of GFC when using a multispectral image issued from medium band filters.

Method	GFC			
	Mean	**median**	**STD**	**Min**
PCA	***0.9970***	***0.9993***	0.0081	0.9604
Wavelets	0.9948	0.9971	***0.0071***	***0.9665***

Table 4: results for the reflectance estimation from camera outputs in the case of multispectral image from medium-band filters.

Discussion

Looking to the results of the first experiment, one can remark that Fourier basis presents the worst performances and presents some artifacts on the boundaries as depicted in Figure 2. **b.** (encircled area); this even we replicate periodically the reflectance samples. The wavelets remedy to this problem thanks to multiresolution analysis and presents therefore good results in terms of GFC and visual comparison. But, the PCA presents the greatest scores for the task of reconstructing samples from the training set. It is natural since PCA derive Smooth basis for smooth data set. For the generalization task, the wavelets basis functions performs better and get the best scores in term of GFC and curves visual comparison even the training set and test set are statistically similar (Macbeth DC and Macbeth CC). We notice that we could use the basis functions derived from the first experiments in the case of wavelets. Wavelets basis are independent from training. The only hypothesis is that

the curves are smooth.
The third experiment shows again the best performance of the wavelets in the task of estimating reflectances from multispectral output system. In the case of multispectral image issued from narrow-band filters, scores for the wavelets are largely superior. That means that PCA is not adapted to reconstruction for this kind of images. In the case of multispectral image issued from medium-band filters, the two methods presents quite similar results. The mean and median are superior for PCA but the standard deviation and the min are superior for Wavelets. That expresses the stability in the results of wavelets.

Conclusion

In this paper, we introduced a new method for spectral reflectance reconstruction using wavelets basis functions. We tested this method in three cases: reconstruction of the training set, generalization and the reconstruction of reflectance from multispectral imaging system. We compare this method to two other methods belonging to the same paradigm: Fourier and PCA. We evaluate the results in terms of GFC and reflectance curves comparison. The proposed method show good and stable performance in all experiments. The future work will concern designing and testing other types of wavelength more adapted to smooth reflectances.

Bibliography

1. Mansouri, F. S. Marzani, P. Gouton, Development of a protocol for CCD calibration: application to a multispectral imaging system, Intl. Journal of Robotics and Automation, Acta Press, 20 (2), 94-100 (2005).
2. A. Ribes-Cortes , Analyse multispectrale et reconstruction de la reflectance spectrale de tableaux de maître, PhD thesis, ENST Paris, december (2003).
3. A. Hosoi, K. Miyata, H. Haneishi and Y. Miyake, Filter Design of Multispectral Camera Based on CCD Sensor Noise Analysis, Proc. Intl. Symposium on Multispectral imaging and Color Reproduction for Digital Archives, Chiba, Japan, 159-162 (1999).
4. F. König, F and W. Praefcke, A multispectral scanner, In Colour Imaging: Vision and Technology, John Wiley & Sons Ltd, 129-144, (1999).
5. G.D Finlayson, P.M. Morovic, Metamer Constrained Colour Correction, Proc. 7th Color Imaging Conference, Scottsdale, Arizona, 26-31 (1999).
6. C. Li and M.R. Luo, The estimation of spectral reflectances using the smoothness constraint condition, Proc. 9th Color Imaging Conference, Scottsdale, Arizona, 62-67 (1999).
7. C. van Trigt, Smoothest reflectance functions. I. Definition and main results, Journal of Optical Society of America - A, 7(12), 1891-1904 (1990).
8. Ribés, and F. Schmitt, A Fully automatic method for the reconstruction of spectral Reflectance curves by using mixture density networks, Pattern Recognition Letters, 24(11), 1691-1701 (2003).
9. D. Connah, , J. Y. Hardeberg and S. Westland, Comparison of linear spectral reconstruction methods for multispectral imaging, IEEE-International Conference on Image Processing (ICIP04), 1497-1500 (2004).
10. L. T. Maloney, Evaluation of linear models of surface spectral reflectance with a small number of parameters, Journal of the Optical Society of America - A, 3 (10), 1673.1683 (1986).
11. J. Y. Hardeberg, F. Schmitt and H. Brettel, Multispectral color image capture using liquid crystal tunable filter, Optical Engineering, 41(10), 2532-2548 (2002).
12. Mansouri, F. S. Marzani and P. Gouton, Neural networks in cascade schemes for spectral reflectance reconstruction , IEEE-International Conference on Image Processing (ICIP05), II, 718-721 (2005).
13. L. MacDonald, S. Westland and D. Liu, Multispectral image encoding and compression. In proceedings of 9th Color Imaging Conference: Color Science, Systems, and Applications, Scottsdale, Arizona, USA, 135-140 (2001).
14. S. Westland and C. Ripamonti, Computational colour Science using Matlab, Chapter 10: Multispectral imaging, John Wiley & Sons eds., (2004).
15. J. Y. Hardeberg, Acquisition and Reproduction of Color Images: Colorimetric and Multispectral approaches, Universal Publishers/dissertation.com, Parkland, Florida, USA (2001).
16. D. Gabor, Theory of communication, J. IEE, 93, 429-457 (1946).